CHAPTER II

A CRITICAL REVIEW OF MECHANICAL BEHAVIOUR OF JOINTED ROCKS

2.1 GENERAL

A critical review of various investigations evince that quite a number of investigators have contributed in developing present state of art on mechanical behaviour of jointed rocks. Various aspects on which these research workers have focussed their efforts can be catagorized as under :

(i) Frictional characteristics of sliding surfaces

(ii) Concept of friction for jointed rocks

(iii) Physical model studies of jointed rock

(iv) Volume change and dilatancy in jointed rock

(v) Yield criteria

2.2 FRICTIONAL CHARACTERISTICS OF SLIDING SURFACES

Tschebotarioff and Welch (1948) performed friction tests between quartz blocks sliding over quartz particles which were first polished and then roughened. They found that while the frictional coefficient for polished mineral particles under disiccator ($CaCl_2$) conditions was 0.106, its value rose to 0.370 for roughened particles.

Ripley and Lee (1961) tested specimens of Sandstone, Siltstone and Shale. The frictional values so measured were corrected for dilation and it was found that coefficient values so obtained were higher for rough surfaces than for ground surfaces.

Frictional characteristics of minerals commonly found in rock have been investigated experimentally by Horn and Deere (1962). The test results revealed that the presence of water on sliding surfaces of minerals greatly increases the frictional coefficient of minerals having massive crystal structures such as quartz and feldspar but decreases the frictional coefficient of minerals having layered lattice structures such as mica and chlorite. The antilubricating action of fluids on massive structured minerals was found to be pronounced when the fluids were polar like water.

RAE (1963) measured coefficient of friction values between Limestone Slider and Sandstone friction wheel and found that after a certain amount of wear the coefficient of friction fell considerably from 0.45 to 0.30.

Parikh (1967) while working on stress dilatancy concept observed the enhancing and diminishing effects of polar and non-polar fluids on coefficient of friction angles of particles of glass ballatoni, bronze balls, quartz or feldspar.

Byerlee (1967) conducted tests on polished surfaces and reported that the coefficient of friction for finely ground surfaces is lower than that for the coarsely ground surfaces.

Hoskins et al (1968) suggested that the tangential stress between sliding surfaces is dependent upon the surface roughness. They found that the coefficient of friction for rough surfaces of trachyte was 0.68 while for polished surfaces it was 0.58.

Einstein et al (1969) compared the Mohr's envelope for sliding along a pre-existing joint with the Mohr's envelope for sliding along a failure surface formed after fracturing which is rougher, for gypsum plaster as a model material. They reported that both the envelopes have the same inclination with the difference that the apparent intercept on the shear stress axis is greater for rougher surfaces.

Studies conducted by Coulson (1970) indicate that surface roughness effectively increases initial friction for all rock types tested like Basalt, Granite, Sandstone, Gneiss, Dolomite, Limestone etc. It also indicates that for smaller normal pressure, the surface damage is slight and roughness affects the residual coefficient of friction. At higher normal pressure, surface damage tends to neutralise the effect of surface roughness.

Proctor et al (1974) used a new interparticle friction device to measure the component of small forces and displacements which occur in one plane at specific time intervals when one particle traverses another. The investigation included artificial particles of glass ballotini, stainless steel balls and natural irregular particles of quartz and feldspar. They concluded as under :

* The value of Ø for a material is not only a function of the material composition of that material but also of the prevailing surface chemistry at the contact point. This chemistry and the ability to control it, is in turn a function of shape and surface roughness as well as ambient experimental conditions.
* Materials with differing crystalline structures respond in different ways to surface chemistry, particularly to water.
* Stick-slip motion is inherent in all single contact friction tests and particularly so for glass ballotini.
* If an investigation of interparticle surface friction is to be related to the shearing behaviour of the mass, then the chemical condition of the surface

being investigated must be representative of that mass.

Hassani and Scobe (1988) conducted direct shear tests on saw cut, artificially roughened and natural discontinuities. Influence of normal stress, strain rate, water and surface roughness on peak and residual strength are studied. For saw cut smooth rock surfaces it is observed that due to presence of water, the percentage reduction in friction angle was within 10 percent. Rate of strain appeared to exert no significant influence on frictional characteristics.

2.3 CONCEPT OF FRICTION FOR JOINTED ROCKS

Goodman (1968) suggested a classification of joints in rock based on normal stiffness (Kn), shear stiffness (Ks) and shear strength (S). The values of (Kn) and (S) are sub-classified into three groups each, such as high, moderate and low. This creates in all 27 classes by permutation and combination. It is stated that joint stiffness and joint strength are independent.

According to Tulinov and Molokov (1971), a thin sand layer as a filler between the hard rocks like Sandstone and Limestone, does not have any significant influence but in case of relatively weak rocks like Clay and Marl, its influence is rather to increase the angle of friction.

Goodman, Heuze and Ohnishi (1972) examined the influence of the thickness (R) of the filling material in Granite and Sandstone joints. It is shown that for very small thickness of the filling materials, there is an augmentation of the strength as a virtue of the geometry of the rough walls of the joint. As the thickness increases, clay filling reduces the strength and at R/t = 3 (where t = mean asperity height) the strength is reduced to that of the filling material. For idealized saw tooth surfaces, Goodman (1969) found the R/t ratio to be 1.5

Barton (1974) has proposed that shear strength of joints filled with a thick layer is basically that of the soil whereas estimating the shear strength of fillings with a thickness less than the roughness amplitude of the joint surface may be problematic since a limited shear displacement will result in a marked stiffning due to increasing rock contact.

Barton (1976) stated that for interlocking rough joint surfaces under low to medium stress levels

$$\tau = \sigma_n \tan\left[20 \log_{10}\left(\frac{\sigma_c}{\sigma_n}\right) + 30\right] \qquad (2.1)$$

For smooth surfaces

$$\tau = \sigma_n \tan \phi_b \qquad (2.2)$$

where,* ϕ_b = basic friction angle

σ_c = unconfined compressive strength

The generalised form of equation (2.1) is given as,

$$\tau = \sigma_n \tan\left[JRC \log_{10}\left(\frac{JCS}{\sigma_n}\right) + \phi_b\right] \qquad (2.3)$$

where, JRC = Joint roughness coefficient which varies from 20 to 0

JCS = Joint wall compressive strength

He further postulated that on saturation rough surfaced joints presumably reduce in strength more than smooth surfaced joints.

----

*The notations used by the original authors have been retained.

Barton et al (1977) have stated that peak shear strength envelopes for non planar rock joints are strongly curved. The real contact area involved during shearing of rock joints may be ranging from 1/10th to 1/100th of the gross contact area. They have tabulated basic friction angles for various rock types which are reproduced in Table 2.1. For weathered rock joints the residual friction angle ϕr may be less than ϕb. Typical rouchness profiles and their roughness numbers are also suggested. It is stated that dilation results in an increase in effective normal stress which results in a large increase in shear strength if the joints are dilatant rather than planar or clay filled. Joint damage coefficient M is defined as

$$M = \frac{JRC \log_{10}\left(\frac{JCS}{\sigma_o}\right)}{d_n} \qquad (2.4)$$

where, dn = maximum dilation angle for given normal stress
General equation for shear strength is given by

$$\tau = \sigma_n \tan(M d_n + \phi_r) \qquad (2.5)$$

Before the onset of shearing a joint that is mated may have a relatively large area of asperities in contact. However, once shearing commences under a given effective normal stress, the contact area begins to reduce. The instant of peak shear strength is reached possibly when the contact area is sufficiently small for the relevant asperities to have reached their limiting state.

Lama (1978) has found that a kaolin layer in a joint, decreases the peak shear strength even when the filler thickness is a small fraction of the asperity height. Other authors such as Jeager (1959), Romero (1968), Goodman (1970), Coulson (1970), Tulinov et al (1971) have demonstrated that the strength and the stiffness of infilled joints change gradually and not abruptly with the relative filler thickness. Kanji (1974) has found that residual shear strength of smooth

TABLE 2.1 : BASIC FRICTION ANGLE FOR VARIOUS ROCKS
Barton et al (1977)

Rock	Moisture	(MN/m^2)	$\emptyset°_b$
Amphibolite	dry	0.1-4.2	32
Basalt	dry	0.1-8.5	35-38
	wet	0.1-7.9	31-36
Conglomerate	dry	0.3-3.4	35
Chalk	wet	0.0-0.4	30
Dolomite	dry	0.1-7.2	31-37
	wet	0.1-7.2	27-35
Gneiss (schistose)	dry	0.1-8.1	26-29
	wet	0.1-7.9	23-26
Granite (f.g.)	dry	0.1-7.5	31-35
	wet	0.1-7.4	29-31
Granite (c.g.)	dry	0.1-7.3	31-35
	wet	0.1-7.5	31-33
Limestone	dry	0.0-0.5	33-39
	wet	0.0-0.5	33-36
	dry	0.1-7.1	37-40
	wet	0.1-7.1	35-38
	dry	0.1-8.3	37-39
	wet	0.1-8.3	35
Porphyry	dry	0.0-1.0	31
	dry	4.1-13.3	31
Sandstone	dry	0.0-0.5	26-35
	wet	0.0-0.5	25-33
	wet	0.0-0.3	29
	dry	0.3-3.0	31-33
	dry	0.1-7.0	32-34
	wet	0.1-7.3	31-34
Shale	wet	0.0-0.3	27
Silstone	wet	0.0-0.3	31
	dry	0.1-7.5	31-33
	wet	0.1-7.2	27-31
Slate	dry	0.0-1.1	25-30

rock soil contacts may be lower than that of the soil alone, its cause is sought in the forced alignment of the clay particles along the narrow failure zone.

Datir (1981) conducted insitu shear tests on natural joints between two lava flows (Intertrapean bed) and on concrete rock (Basalt) interface. It is observed that the ratio of thickness of filling material to the height of asperity was more than 3 and hence the friction angle (Ø) of the joint was found to be equivalent to the residual angle of internal friction (Øf) of the filling material which was estimated to be 1.5 times the basic friction angle ($\emptyset_\mu$) of that material. The peak shear strength of concrete-rock interface was found to be of the form

$$\tau = \sigma \tan\,(\phi_\mu + i) \qquad (2.6)$$

where, i was the average dilation angle.

For working out cohesion of such surfaces following form was observed :

$$C = \tau\ \text{peak} - \tau\ \text{residual} \qquad (2.7)$$

All expressed in same units.

Shah (1983) conducted triaxial compression tests on cylindrical samples of Basalt having saw cut joint at 54.8° with horizontal, filled with gouge composed of mix of bentonite and cement in different proportions. It was found that the behaviour of the sample exhibited the shear characteristics of gouge material only and did not indicate effect of parent rock.

Shah (1984) conducted triaxial compression tests on cylindrical samples of Basalt having saw cut joint at 30°, 45° and 54.8° with horizontal, filled with gouge of cement-sand mortar in proportion of 1 : 2, 1 : 3 and 1 : 4. The joint thickness was 2 mm. The behaviour of jointed rock filled with gouge was found to exhibit the shear characteristics of the gouge material.

Hassani et al (1985) observed that two distinct portions of failure envelope exist for rock joints with rough surfaces. At low normal stress range, the coefficient of peak angle of friction reduces with increase in normal stress. However, at higher normal stress, the angle becomes independent of normal stress. Authors have further observed that general mode of predicted envelopes following Barton (1971) indicates an over estimation of the shear strength. It is suggested that work on developing power curve analysis as a predictive approach should be taken up.

Turk et al (1985) have proposed a method for the estimation of rock joint roughness angle i. They have concluded that the dilation angle is specimen size dependent and experimental values are higher for small specimens than those determined for large surfaces. The effect of increase in normal stress is to decrease the dilation angle. It is further concluded that even after large shear deformation, dilation can still occur after the peak shear stress is reached.

Gandhi (1986) reported conventional triaxial tests conducted on cylindrical samples having gouged saw cut joints. The joints were filled with cement-sand mortar of 2 mm thickness and cement-bentonite gouge of 3 mm thickness. It is postulated that energy dissipated in basic friction is that involved in sliding at a critical orientation of 45 + $\emptyset_{\mu}/2$ to the major principal plane and the excess energy towards dilation is in the process of sliding at an orientation deviating from the critical orientation. Therefore the phenomenological parameter of dilatancy is the ratio of tangents of joint orientation to the critical orientation which is also equivalent to the ratio of lateral strains to the axial strains at the point of failure. This means

$$D = \left(1 - \frac{d\left(\frac{\Delta V}{V}\right)}{d\varepsilon_1}\right) = \frac{\tan\alpha}{\tan(45 + \phi_\mu/2)} \qquad (2.8)$$

where, D is the dilatancy parameter and $(\Delta v/v)$ is the volumetric strain.

On consideration of dilatancy it is observed that the effect of joint orientation is only on the cohesion parameter while the friction parameter remains equivalent to the basic friction angle irrespective of the joint orientation. The derived failure criterion is the Mohr-Coulomb criterion in which stresses have been modified for dilatancy as under :

$$\tau_f = C^* + \sigma_f \tan\phi_\mu \qquad (2.9)$$

where, c* is an intercept inclusive of energy in excess of basic frictional energy.

Dave (1987) conducted direct shear tests on saw cut joints created in Basalt, filled with gouge of cement sand mortar of different proportions in a thickness of 2 mm. It is observed that shear strength of unfilled joints is greater than that of the filled joints. The shear strength of filled joints reduces with the reduction in the strength of the gouge material.

Shah (1987) conducted cyclic direct shear tests on saw cut joint created in basalt, filled with gouge of cement sand mortar of different proportions, in a thickness of 2 mm. The observations are similar to those of Dave (1987).

Barton (1988) has stated that quite accurate predictions of peak shear strength and dilation characteristics of rock joints are possible. He advocated following basic equations describing the friction angle (ϕ_m) and the dilation angle (d_m) mobilised at any given shear displacement, based on the concept of mobilized roughness (JRC_m)

$$\phi_m = JRC_m \log\left(\frac{JCS}{\sigma_n}\right) + \phi_r \qquad (2.10)$$

and
$$d_m = \frac{1}{2} JRC_m \log\left(\frac{JCS}{\sigma_n}\right) \qquad (2.11)$$

The displacement (δ_{peak}) needed to reach peak shear strength is given as

$$\delta_{peak} = \frac{L_n}{500}\left(\frac{JRC}{L_n}\right)^{0.33} \qquad (2.12)$$

where, Ln = Sample size or insitu block size (spacing between cross-joints) in m

JRCn = Joint roughness coefficient of joints of length Ln

Following equations are advocated for stress transformation

$$\sigma_n = \frac{1}{2}(\sigma_1 + \sigma_2) - \frac{1}{2}(\sigma_1 - \sigma_2)\cos[2(\beta + d_m)] \qquad (2.13)$$

$$\tau = \frac{1}{2}(\sigma_1 - \sigma_2)\sin[2(\beta + d_m)] \qquad (2.14)$$

where, σ_1 and σ_2 are the principal biaxial stress components and σ_n and τ are the normal and shear stress components. β is the angle between joint plane and major principal stress.

2.4 PHYSICAL MODEL STUDIES OF JOINTED ROCKS

Brown (1970) carried out a series of triaxial tests of 4" x 4" x 8" samples made up of assemblies of 1 inch cubes of plaster arranged such that three sets of mutually perpendicular joint planes were formed as shown in Fig. 2.1. Model material used was gypsum plaster. It was observed that

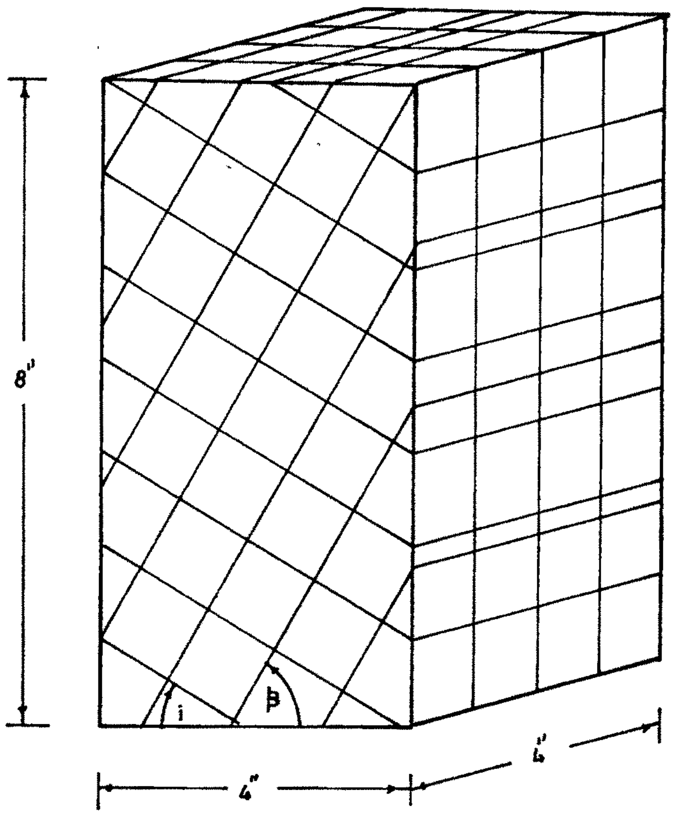

FIG: 2·1 BLOCK-JOINTED SAMPLE GEOMETRY (Barton 1970)

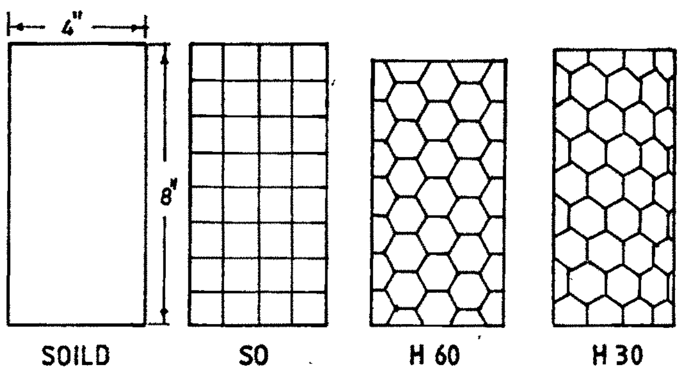

FIG: 2·2 SPECIMEN CONFIGURATIONS (Einstein et al 1973) mechanical behaviour of even the most simple jointed rock system was markedly different from that of the unjointed parent material. Shear strength envelopes having a zero cohesion intercept were obtained, from those tests in which failure was through the model material rather than by slip on a joint surface. A power law was fitted to the test results.

Barton (1972) used a combination of red lead-sand/ bellotini-plaster-water as a model material. A method for producing mating tension fractures in weak brittle model material was described. Direct shear tests were conducted on model tension joints. It was observed that shear stiffness was both normal stress and size dependent. There was an inverse proportionality between test dimension and shear stiffness, for a given normal stress. The normal stiffness was found to be dependent on the preconsolidation or virgin normal stress level. It was observed that a joint had no shear strength until displaced slightly.

Einstein et al (1973) used a model material consisting of a mixture of gypsum plaster, diatomaceous earth and water. A prismatic jointed specimen of 2" x 4" x 8" size was chosen. The joint configurations are shown in Fig. 2.2. Triaxial tests and direct shear box tests were conducted. Following conclusions were drawn :

* The upper limit of the relation between shear strength and normal stress of the jointed mass is defined by the Mohr envelope for the intact material; the lower limit is defined by the Mohr envelope for sliding along a smooth joint surface.

* At low confining pressure the model material fails in a brittle manner and at high confining pressure, the material fails in a ductile manner.

Kutter (1980) conducted direct shear box tests on artificially prepared rock joints. Three types of surface roughnesses namely diamond saw cut surfaces, sand blasted saw cut surfaces and tensile fractured surfaces were tested. Three types of filler materials, viz. fine quartz sand, a silty clay and a sand clay mixture were used. Thickness of soil layer was varied from 2 ± 0.2 mm to 4 ± 0.4 mm. Following relation is observed :

$$\tau_{corrected} = \sigma \tan\left[\arctan \frac{\tau_{measured}}{\sigma} + i\right] \qquad (2.15)$$

It was observed that for soft filled joints, the shear strength of samples was equal to or higher than that of the filler material and for smooth filled joints, it was close to that of the filler material. For thicker layer of filling material the shear strength of samples was close to that of the soil.

Bandis et al (1981) conducted direct shear tests on various sized samples of replicas of joint surfaces. The material used for casting model joints consisted of a mixture of silver sand, calcined alumina, barytes, plaster of paris and water. It was observed that under a given normal load σ_n, complete or partial damage of asperities contribute a shearing or failure component $\dot{S}_A$ to the peak fractured resistance ($\emptyset$ p) as under :

$$\phi_p = \text{peak} \arctan\left(\frac{\tau}{\sigma_n}\right) = \dot{\phi}_b + \dot{d}_n + \dot{S}_A \qquad (2.16)$$

Knox et al (1983) examined the influence of the occurence of weaker strata in layered jointed rock model. The model material used were light weight concrete and gypsum mortars. The models were constructed from blocks of these materials. The load-settlement characteristics, bearing capacity, pattern of deformation amd modes of failure are observed. Results are compared with those predicted by F.E. analysis. No obvious correlations between the two are discovered.

Venkatachalam (1985) conducted direct shear tests on model of rock joints. Model material used consisted of a mix of wheat flour and methanol. Following findings are reported :

* Relationship is curvillinear at low normal stresses but linear at high normal stresses.

* There is a sudden drop in shear strength after a certain JRC value. The breakage of asperity brings down the effective JRC and causes reduction in strength.

* Total shear strength is divided into sliding, dilatant and shearing components.

Herdocia (1985) conducted a series of large scale laboratory direct shear tests on identical replicas of a natural joint surface. The effect of normal stress as well as cyclic loading in shear over the response of joint were studied. Araldite epoxi resin filled with sand ballast was used to cast replicas of the same natural joint. The joint surface was taken from a bedding plane of slate. Profiles were surveyed by a profilometer. It was observed that cycles of stress did not produce any major changes in the shape of the shear stress versus shear deformation curve. Pre-peak portion of the shear stress versus shear deformation curve can be satisfactorily approximated by using a simple hyperbolic equation of the form

$$\tau = \frac{\delta_s}{(m + n \times \delta_s)} \tag{2.17}$$

where, m = intial shear compliance

n = reciprocal of the horizontal limit of the hyperbola on the maximum shear stress

Under cyclic loading in shear, the unloading and subsequent loading followed nearly the same path. The maximum dilation rate was recorded at displacement corresponding to that of the peak shear stress. The dilation angle at the peak shear stress did not decrease significantly with the increase in normal stress.

Hassani et al (1985) conducted extensive direct shear testing of saw cut, artificially roughened and natural discontinuities. Influence of normal stress, strain rate, water and surface roughness; on peak and residual shear strength are studied. For saw cut, smooth rock surfaces it was observed that due to presence of water the percentage reduction in friction angle was within 10%. Rate of strain appeared to exert no significant influence on frictional characteristics. Artificial discontinuities with varying surface roughness using idealized asperities were actually machined in rock. These comprised grooves and mating ridges. Peak shear strength curve was found to be bilinear. Progressive failure of asperities appeared to be responsible for less marked increase in peak shear strength with increase in asperity frequency.

2.5 VOLUME CHANGE AND DILATANCY IN JOINTED ROCKS

Casagrande (1936) first described the influence of dilatancy on the drained friction angle of sands while Rowe (1962), Lee and Seeds (1967) and others clarified the relative role of dilatancy, particle arrangement and particle crushing. Bjerrum (1970) expressed the view that the degree of dilatancy of a fractured rock mass is a relevant rock property for design of support system.

Brace et al (1966) have suggested that in laboratory testing, an axial stress-volumetric strain curve is the most sensitive indicator of initiation and subsequent growth of cracks. The tests showed that rocks exhibit a marked increase in volume when stressed near their maximum load carrying capacity. They referred to this phenomenon as dilatancy and ascribed it to the development of cracks.

Crouch (1970) presented a method of determining volumetric strains in cylindrical test specimen. In triaxial testing the volume of a fluid filled pressure vessel must be adjusted to compensate for lateral expansion of the specimen, if the fluid is to be kept at constant pressure. The amount by which the volume has to be adjusted is a direct measure of the lateral component of the volumetric strain.

Ladyani and Archambault (1969) formulated a curved Mohr envelope typical of the shear strength of a rough clean joint.

$$\tau = \frac{\sigma(1-a_s)(\dot{V}+\tan\phi_\mu)+a_s\eta C_o \frac{m-1}{m} \times \left(1+\frac{n\sigma}{\eta C_o}\right)^{\frac{1}{2}}}{1-(1-a_s)\dot{V}\tan\phi_\mu} \qquad (2.18)$$

where, v = dilation rate at peak shear stress = dv/du

a_s = proportion of total area which is sheared through asperities

= degree of interlocking at peak load

C_o = compressive strength of rock

n = ratio of tensile to compressive strength

m = $(1+n)^{1/2}$

They also suggested that the dilatancy rate would decrease with the fourth power of the normal pressure.

$$\dot{V} = \frac{dv}{du} = \tan i_o \left[\left(1-\frac{\sigma}{\sigma_t}\right)^{K_2} \right] \qquad (2.19)$$

with K_2 = 4

io = dv/du at low normal stress

Bordia (1971) observed that the failure strength is proportional to dilatancy at the critical fracture point σcr. If there is no dilation, the failure strength will be equal to the fracture initiation strength, which suggests the addition of a dilatancy hardening term to express the failure strength in terms of failure initiation strength. This relationship is expressed as

$$\sigma_f = 10^3 d_{cr} \ \sigma_i + \sigma_i \tag{2.20}$$

It was observed that dilatancy was due to stress concentration and the consequent stress-strain distribution.

Goodman el al (1972) observed that a dilatant joint tested in direct shear apparatus under constant normal deformation will have higher friction angle than one tested under constant normal stress. This leads to introduction of dilatancy in analysis through an adjustment of friction angle. However, because the dilatancy also affects the amount of deformation of joints, a stress analysis cannot satisfactorily duplicate dilatancy effects, merely by adjusting friction angle. They further indicated idealized behaviour of dilatancy versus normal pressure assumed by them. The dilatancy angle i is given by

$$\tan^{-1}\left(\frac{dv}{du}\right) = i = (i_o - i_m)\left[\frac{\sigma_m - \sigma}{\sigma_m}\right]^{\frac{1}{2}} + i_m \tag{2.21}$$

Edmond et al (1972) have observed that the deformation of rocks can be accompanied by substantial volume changes even in the range of macroscopically ductile behaviour. These large volume changes are attributed to changes in the pore pressure, or grain arrangement or to the development of the internal cracking.

Schneider (1976) studied friction and deformation behaviour of rock joints. On the basis of the results of friction tests on models a friction law has been proposed as under :

$$\tau = \sigma \tan\left(\phi + i_o e^{-K_1 \sigma}\right) \tag{2.22}$$

In this law the dilation angle i at zero normal load at the immediate beginning of the dilation movement decreases exponentially with increasing normal stress. Coefficient K_1 varies from material to material type. The relationship between i and io is given as

$$i = i_o \exp(-K\sigma_n) \qquad (2.23)$$

where, i is the effective dilation angle under positive normal stress and K is an empirical constant.

He has also shown the relationship between maximum dilatancy and normal stress as

$$h = h_o e^{-K\sigma} \qquad (2.24)$$

where, ho is the maximum dilatancy at zero normal stress and K is a constant. K is related with the tensile strength of the material as

$$K = a(\sigma d)^{-b} \qquad (2.25)$$

$$d = 1\ cm^2/Kp \qquad (2.26)$$

where, a and b are coefficients for each joint type.

Heuze (1979) presented a theory to predict the effects of dilation on the behaviour of rock structures. According to him

$$\tau = A\sigma + B\sigma^2 + C\sigma^3 \qquad (2.27)$$

where, $A = \tan \phi_p$

$$B = \frac{3C_p^*}{\sigma_c^2} - \frac{2(\tan\phi_p - \tan\phi_R)}{\sigma_c}$$

$$C = \frac{-2C_p^*}{\sigma_c^3} + \frac{(\tan\phi_p - \tan\phi_R)}{\sigma_c^2}$$

c_p^* = apparent cohesion intercept of the residual envelope

Instantaneous dilation angle δ is given by

$$\delta = A\tan(A + 2B\sigma + 3C\sigma^2) - \phi_R \qquad (2.28)$$

Pender et al (1983) postulated a mathematical model of dilatant behaviour. The dilatant volume change is calculated by relating it to octahedral shear stress. It is assumed that the rock mass behaves as a conventional linear elastic material with the addition of a dilatant contribution. The constitutive relationship expressed in incremental form is

$$dV_{oct} = \frac{d\sigma_{oct}}{K} - \frac{d\tau_{oct}}{D} \qquad (2.29)$$

and

$$d\gamma_{oct} = \frac{d\tau_{oct}}{G} \qquad (2.30)$$

where, dV_{oct} = octahedral volumetric strain increment
K = bulk modulus
G = shear modulus
D = modulus of dilatancy

Authors have stated that the initial part of the volumetric strain curve can be modelled as a conventional isotropic elastic material with increasing Poisson's ratio. However, once the minimum volume is passed a Poisson's ratio greater than 0.5 would be required to model the volume change behaviour. To get over this difficulty the dilatant term has been introduced.

2.6 YIELD CRITERIA

2.6.1 General

Establishment of the mathematical expression known as the 'yield criterion' has to be done based on experimental observations. Original experimental work was done on metals and hence the development of this subject started with metal plasticity. In view of the complexities involved in the yielding of materials under three dimensional state of stress, it is convenient to define a scalar function, F, as the yield criterion, such as

$$F = F(\sigma_{11}, \sigma_{22}, \sigma_{33}, \sigma_{12}, \sigma_{23}, \sigma_{31}) \qquad (2.31)$$

It can also be expressed in terms of principal stresses and their directions, such as

$$F = F(\sigma_1, \sigma_2, \sigma_3, n_1, n_2, n_3) \qquad (2.32)$$

where, n_1, n_2, n_3 are the direction cosines of the principal stresses.

If the material is assumed to be isotropic the yield criteria reduces to

$$F = F(\sigma_1, \sigma_2, \sigma_3) \qquad (2.33)$$

This can also be expressed more conveniently in terms of the invariants of the stress tensor as follows

$$F = F(J_1, J_2, J_3) \qquad (2.34)$$

Some popular yield criteria are as under.

2.6.2 Non Frictional Yield Criteria

(1) Von Mises Yield Criterion

This criterion was suggested by Von Mises in 1913 and is known as the distortional energy theory. According to this theory yielding will initiate when the second invariant of the deviatoric stress tensor reaches a certain value. Actually this criterion assumes that yielding begins when the distortional energy reaches a value that is equal to the distortional energy at yield in simple tension. According to this criterion,

$J_{2D} < K^2$ if the material is in the elastic state

$$\text{and } J_{2D} = K^2 \quad \text{if the material is yielding} \tag{2.35}$$

Here K is a material constant.

In general form the Von Mises criterion can be expressed as

$$\frac{1}{6}\left[(\sigma_{11}-\sigma_{22})^2+(\sigma_{22}-\sigma_{33})^2+(\sigma_{33}-\sigma_{11})^2\right]+\sigma_{12}^2+\sigma_{23}^2+\sigma_{31}^2=K^2 \tag{2.36}$$

In the principal stress space it can be written as

$$\frac{1}{6}\left[(\sigma_1-\sigma_2)^2+(\sigma_2-\sigma_3)^2+(\sigma_3-\sigma_1)^2\right]=K^2 \tag{2.37}$$

This criterion represents a circle of radius $\sqrt{2/3}\,\sigma_Y$ on the π plane (Fig. 2.3).

(2) Tresca Yield Criterion

According to this criterion yielding will initiate when the maximum value of the extreme shear stress is reached. In this theory, yield strength in tension and compression have been assumed to be equal which is a limitation for many materials. The yield criterion is

$$\sigma_2 - \sigma_1 = \sigma_Y \tag{2.38}$$

According to this criterion the yield stress in pure shear is equal to half of σ_Y. This criterion can be represented

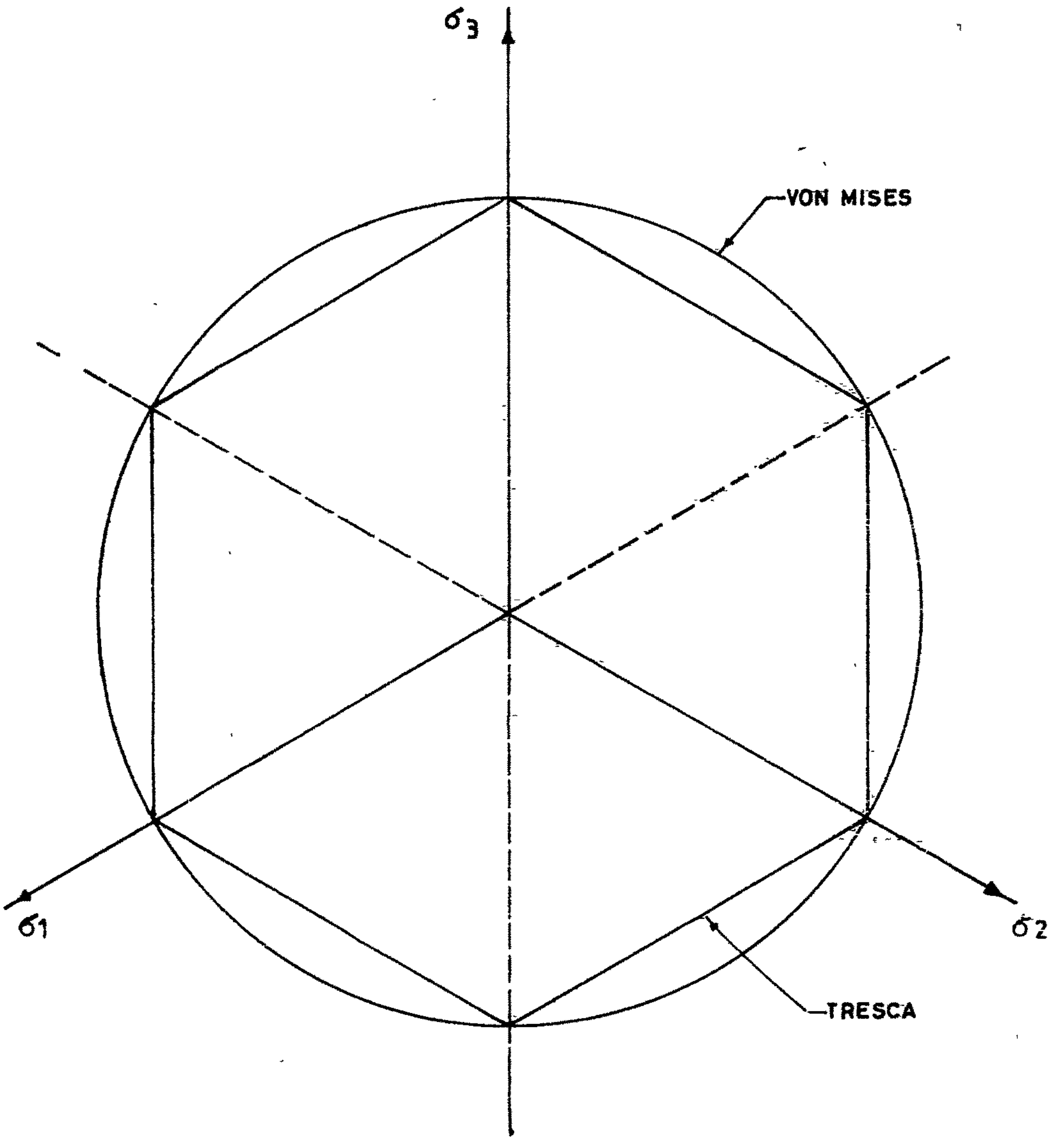

FIG: 2·3 PROJECTIONS OF VON MISES AND TRESCA CRITERIA ON π PLANE by a regular hexagon on π plane (Fig. 2.3).

2.6.3 Frictional Yield Criteria

The behaviour of geologic media is quite different from that of metals. Yield criteria developed for metals assume that the strength of the material is independent of the hydrostatic stress. These types of materials are called non frictional materials. Geologic materials exhibit frictional characteristics and therefore frictional yield criterion are developed for geologic materials.

(1) Mohr Coulomb Failure Criterion

According to this criterion, the shear strength increases with increasing normal stress on the failure plane, i.e.

$$\tau = C + \sigma \tan\phi \tag{2.39}$$

or it can also be written as

$$\frac{\sigma_1 - \sigma_3}{2} = \frac{\sigma_1 + \sigma_3}{2} \sin\phi + c\cos\phi \tag{2.40}$$

or $$\sqrt{\left(\frac{\sigma_{11} - \sigma_{33}}{2}\right)^2 + \sigma_{12}^2} = \frac{\sigma_{11} + \sigma_{33}}{2} \sin\phi + c\cos\phi \tag{2.41}$$

Projection of this criterion on π plane is an irregular hexagon as shown in Fig. 2.4. An alternative form of this criterion is

$$f = J_1 \sin\phi + \sqrt{J_{2D}} \cos\phi - \frac{\sqrt{J_{2D}}}{3} \sin\phi \sin\theta - \cos\phi = 0 \tag{2.42}$$

where, $\theta = -\frac{1}{3} \sin^{-1}\left(\frac{-3\sqrt{3}}{2} \cdot \frac{J_{3D}}{J_{2D}^{1/2}}\right)$

and $-\frac{\pi}{6} \leq \theta \leq \frac{\pi}{6}$

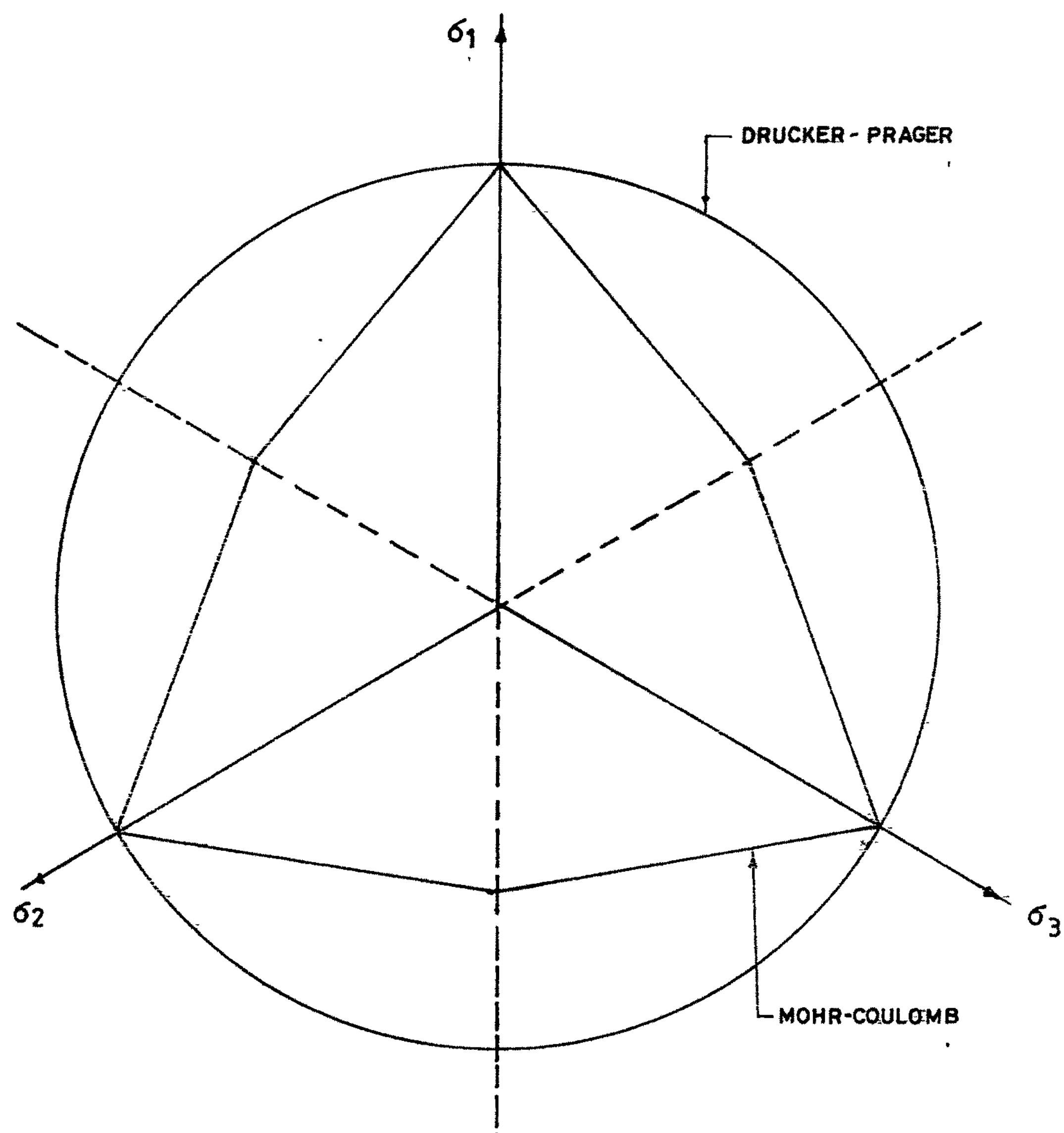

FIG: 2·4 PROJECTIONS OF MOHR COULOMB AND DRUCKER PRAGER CRITERIA ON π PLANE

(2) Drucker Prager Criterion

The generalized criterion can be written as

$$f = \sqrt{J_{2D}} - \alpha J_1 - K = 0 \qquad (2.43)$$

where, α and K are positive material parameters.

When failure envelope is plotted on $J_1 - \sqrt{J_2 D}$ space, slope and intercept of failure envelope gives values of α and K (Fig. 2.5). For conventional triaxial compression

$$\alpha = \frac{2 \sin \phi}{\sqrt{3}(3 - \sin \phi)} \qquad (2.44)$$

and

$$K = \frac{6 c \cos \phi}{\sqrt{3}(3 - \sin \phi)} \qquad (2.45)$$

Projection of this criterion on π plane is a circle as shown in Fig. 2.4.

2.7 CONCLUDING REMARKS

From the research review presented it is seen that most of the research work on jointed rock has been done in last two decades. A number of investigators have put forward different theories and concepts for understanding the mechanical behaviour of jointed rock. However, conclusions of many of them are localised and therefore can not be generalized for application. Besides very few have focussed their attension on the inclusion of dilation parameter in real terms in estimating the shear strength of jointed rock. It is therefore necessary to evolve a generalized criterion applicable to all situations in jointed rock. It is also necessary to account **properly for** the dilation or the volume change - through a realistic parameter - for its inclusion in the constitutive relationship of jointed rock.

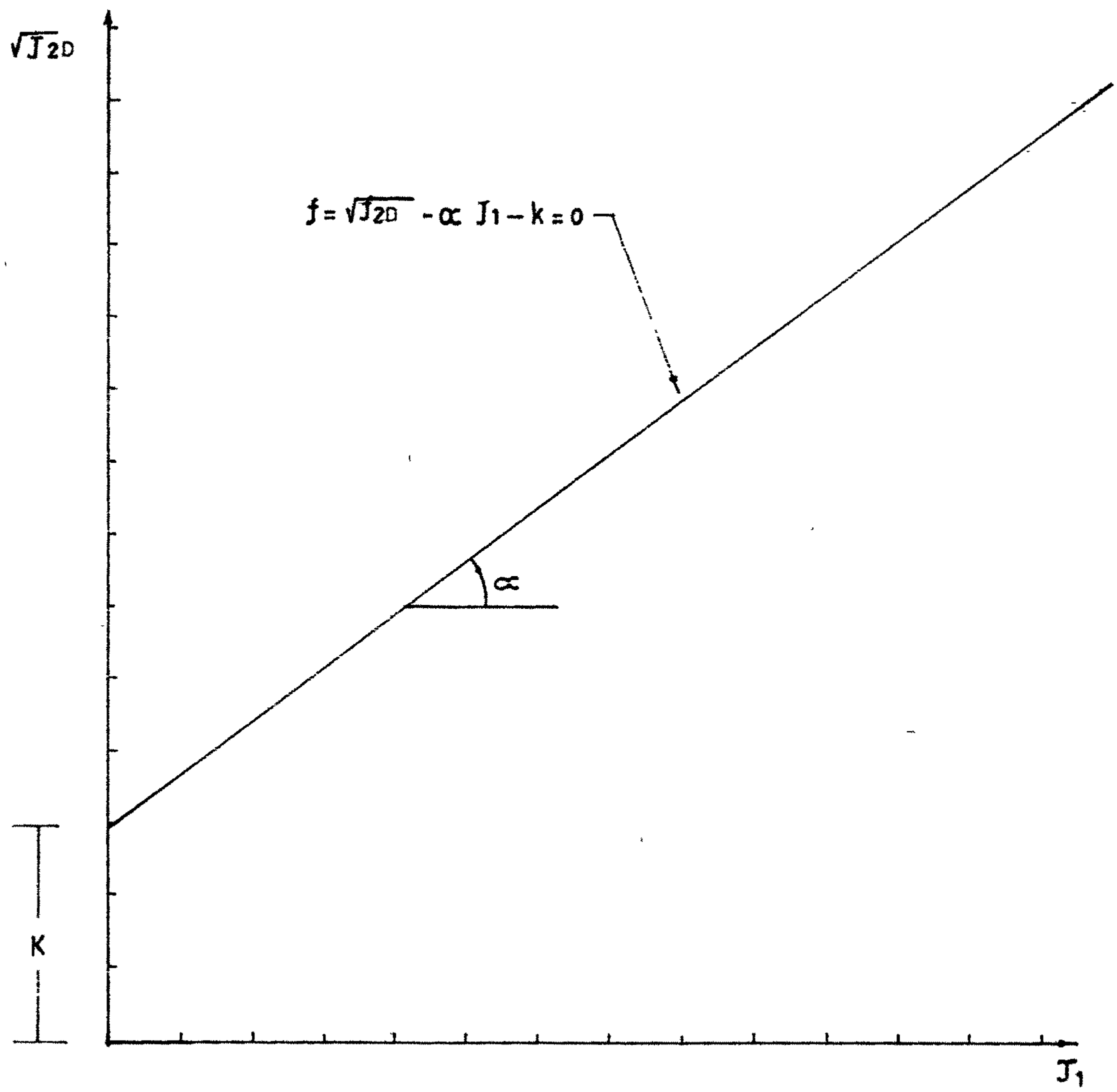

FIG: 2·5 DRUCKER PRAGER CRITERION ON $J_1 - \sqrt{J_{2D}}$ PLANE